Regular Article

PHYSICAL CHEMISTRY RESEARCH
Published by the
Iranian Chemical Society
www.physchemres.org
info@physchemres.org

Phys. Chem. Res., Vol. 11, No. 4, 897-912, December 2023
DOI: 10.22036/pcr.2022.361112.2189

A Numerical Investigation of the Thermal Transport Properties of Argon + Hydrogen Plasma Working Gases in the Presence of Various TiO_2 Precursor Solutions

K.T. Simfroso[a,b], A.Q. Liboon, Jr.[c] and R.T. Candidato, Jr.[a,b,*]

[a]*Materials Science Laboratory, Department of Physics, MSU- Iligan Institute of Technology, Andres Bonifacio Ave., Tibanga, Iligan City 9200 Philippines*

[b]*Premier Research Institute of Science and Mathematics, MSU- Iligan Institute of Technology, Andres Bonifacio Ave., Tibanga, Iligan City 9200 Philippines*

[c]*Jose Rizal Memorial State University- Tampilisan Campus, Znac, Tampilisan, Zamboanga del Norte, 7116, Philippines*

(Received 7 September 2022, Accepted 20 December 2022)

We reported a numerical investigation of the thermal transport properties of argon (Ar) + hydrogen (H_2) plasma working gases such as the dynamic viscosity and thermal conductivity under the presence of various titania (TiO_2) precursors. Titanium nitride (TiN), titanium isopropoxide (TIP), and titanium butoxide (TB) mixed with water or ethanol having molar concentrations of 0.5 M, 0.75 M, and 1 M were used. Results showed that the dynamic viscosity value of the plasma jet was decreased by the presence of TB and TIP precursor solution, notably for high concentration and feed rate, indicating a decrease in the momentum of particles inside the plasma jet. On the other hand, the thermal conductivity increased when TB and TIP solutions were injected and were influenced by the solution concentration and feed rate. This was attributed to the additional hydrogen ions from TIP and TB precursors, which are absent in the TiN precursor, that increase the number of mobile atomic species. From these transport properties, the modified ability of heating factor of Ar + H_2 plasma was calculated. The highest values were obtained for the compositions, including the TB precursor solution, which is 2 to 3.5 times higher than pure Ar + H_2 plasma working gases.

Keywords: Ability of heating factor, Dynamic viscosity, Plasma working gases, Solution precursor plasma spraying, Thermal conductivity

INTRODUCTION

The solution precursor plasma spray (SPPS) process is an emerging method that offers a single-step deposition of various nanostructured coatings [1-3]. This technique uses molecularly mixed precursors as feedstock, thus, avoiding tedious nano-powder and suspension preparation processes [4]. Many recent works have been reported employing SPPS for development materials intended for desired applications such as protective and thermal barrier coatings [5,6], gas sensors [7], and biomaterial coatings [8]. However, only limited works were presented about photocatalytic coatings like titania (TiO_2) [9,10] and this could be due to the difficulty of preparing precursor solution and obtaining high-phase purity titania coating.

In SPPS, the resulting deposits have unique particle morphologies and are known to depend on the thermal history of droplets undergoing physico-chemical transformations inside the plasma jet. Experimental examination of the thermo-physical changes of droplets is still a difficult task because of the quick residence time of droplets inside the plasma jet and also because of the high temperature and radiative properties of the plasma jet. One

*Corresponding author. E-mail: rolandojr.candidato@g.msuiit.edu.ph

way to possibly understand and picture out the process of droplet transformation during the spraying experiment is *via* numerical analysis.

Several research works on numerical modeling of the transformation of droplets in SPPS have been reported with emphasis on zirconium hydrochloride solution, lanthanum-hexahydrate solution, and cerium nitrate solution [11-14]. However, the analysis of thermodynamic properties is equally important to be understood as they play a significant role during the heat and momentum transfer between solution droplets and plasma working gases. It is given that during plasma spraying, the evaporation of liquid from the precursor solution affects the composition of plasma working gases, thereby changing the thermal transport properties.

Experimental studies of Chen *et al.* [15-17] and Wen *et al.* [18] focused only on obtaining TiO_2 coatings from TIP solution precursor and TiO_2 powder + water feedstocks using Ar + H_2 plasma via SPPS process. For the determination of transport properties, recent related studies found mostly deal with two-temperature plasma [19-22] especially 2T Ar + H_2 plasma with the presence of other compounds [23]. Murphy *et al.* [24], Wang *et al.* [25], Li *et al.* [26], Lisong *et al.* [27], and Colonna *et al.* [28], however, worked on the different types of plasma, though Murphy and Tam [24] worked on Ar alone and compared it with Xe and Kr plasma. The recent papers of Miao *et al.* focused on the vortex characteristics and gas-dynamic fields of Ar + H_2 inductively-coupled plasma [29] and showed the involvement of Ar + H_2 in LTE with the presence of quartz [30]. Pateyron *et al.* [31] and Carpio *et al.* [14], on the other hand, studied numerically the influence of water and ethanol and various zirconia precursor solutions, respectively, on the transport properties of Ar + H_2 plasma working gases.

The current work aims to study the effect of various precursor solutions that can be used for the synthesis of TiO_2 coatings on the thermal transport properties of the plasma working gases. Besides, the effect of the type of precursor, feedstock flow rate, solvent and solution concentration are also analyzed. TiO_2 is particularly selected in this work since it is an important and known photocatalytic ceramic material and SPPS could be a way to deposit it with nanometric or sub-micron features which could be useful for environmental pollution remediation, such as air and water purification, photocatalytic degradation of harmful and toxic organic pollutants and for photocatalytic water splitting. The understanding of the interaction between solution precursors and plasma may be a step forward in controlling and optimizing the spray processes involved. The present paper analyzes three different TiO_2 precursor solutions at varied concentrations and injection feed rates and solvents.

EXPERIMENTAL APPROACH

TiO_2 Precursor Solutions and Operational Spray Parameters

A mixture of argon (Ar) and hydrogen (H_2) gases was used as the plasma working gas where Ar is the primary gas and H_2 is the secondary one. The flow rates of Ar and H_2 gas were set at 45 slpm and 5 slpm, respectively. The following TiO_2 solution precursors; titanium nitride (TiN), titanium isopropoxide (TIP), and titanium butoxide (TB), are mixed with water and ethanol to obtain the desired solution concentrations, which then served as the solution feedstocks to be injected in the plasma jet. The effects of the solution concentration on the transport properties of Ar + H_2 plasma working gases as well as the feedstock feed rate were evaluated. The different feedstock concentrations and feed rates considered in the calculations are presented in Table 1 while other spray parameters remained constant. The chemical equation for each precursor is expressed as follows: Titanium nitride (TiN) using water as solvent:

$$2TiN + 4H_20 \rightarrow 2TiO_2 + 2NH_3 + H_2 \quad (1)$$

Titanium isopropoxide (TIP) using water and ethanol as solvents:

$$Ti(OC_3H_7)_4 + 4H_2O \rightarrow Ti(OH)_4 + 4C_3H_7OH \quad (2)$$

$$Ti(OH)_4 \rightarrow TiO_2 + 2H_2O \quad (3)$$

$$Ti(OC_3H_7)_4 + 4CH_3CH_2OH \rightarrow Ti(OCH_2CH_3)_4 + 4C_3H_8O \quad (4)$$

$$Ti(OCH_2CH_3)_4 \rightarrow TiO_2 + \text{hydrocarbons} \quad (5)$$

Table 1. Type of Precursor Solution, Solution Concentration, and Injection feed Rates Considered in the Estimations of the Thermal Transport Properties

Precursor Type	Solvent	Legend	Concentration (M)	Feed rate (ml min^{-1})
Titanium nitride (TiN)	Water	TiN1	0.5	30
		TiN2	0.5	50
		TiN3	0.75	40
		TiN4	1.0	30
		TiN5	1.0	50
Titanium butoxide ($Ti(OC_4H_9)_4$	Water	TB + water1	0.5	30
		TB + water2	0.5	50
		TB + water3	0.75	40
		TB + water4	1.0	30
		TB + water5	1.0	50
Titanium isopropoxide ($Ti(OC_3H_7)_4$	Water	TIP + water1	0.5	30
		TIP + water	0.5	50
		TIP + water3	0.75	40
		TIP + water4	1.0	30
		TIP + water5	1.0	50
Titanium butoxide ($Ti(OC_4H_9)_4$	Ethanol	TB + eth1	0.5	30
		TB + eth2	0.5	50
		TB + eth3	0.75	40
		TB + eth4	1.0	30
		TB + eth5	1.0	50
Titanium isopropoxide ($Ti(OC_3H_7)_4$	Ethanol	TIP + eth1	0.5	30
		TIP + eth2	0.5	50
		TIP + eth3	0.75	40
		TIP + eth4	1.0	30
		TIP + eth5	1.0	50

Titanium butoxide (TB) using water and ethanol as solvents:

$$Ti(OC_4H_9)_4 + 4H_2O \rightarrow Ti(OH)_4 + 4C_4H_9OH \quad (6)$$

$$Ti(OH)_4 \rightarrow TiO_2 + 2H_2O \quad (7)$$

$$Ti(OC_4H_9)_4 + 4CH_3CH_2OH \rightarrow Ti(OCH_2CH_3)_4 + 4C_4H_{10}O \quad (8)$$

$$Ti(OCH_2CH_3)_4 \rightarrow TiO_2 + \text{hydrocarbons} \quad (9)$$

The use of water is very economical based on initial studies and is viable to perform SPPS. Ethanol is also used because mostly metal alkoxides are immiscible in water. The simplest way to avoid precipitation and fast reaction, alcohol is employed instead of water. For TiN, only water was used as solvent considering that the chemical reaction between ethanol and TiN is difficult to establish.

Estimation of Thermal Transport Properties

The first step in obtaining transport coefficients was the determination of species composition of thermodynamic equilibrium. The calculation of equilibrium compositions using the free software is based on the minimization of Gibbs free energy described by White *et al.* [32]. The chemical composition of the different plasma mixtures was deliberated from the flow and feed rates of Ar, H_2, and TiO_2 precursor solution. There are 68 species considered: e^-, C^-, C_2^-, H^-, OH^-, O^-, O_2^-, Ti^-, Ar^+, C^+, CH^+, CHO^+, CO, CO_2^+, H^+, O^+, OH^+, Ti^+, Ar^{2+}, O^{2+}, Ar^{3+}, Ar^{4+}, Ar, C, CH, CHO, CHO_2, CH_2, CH_2O, CH_2O_2, CH_3, CH_3O, CH_4, CH_4O, CO, CO_2, C_2, C_2H, C_2H_2, C_2H_2O, $C_2H_2O_2$, C_2H_4, C_2H_4O, $C_2H_4O_2$, C_2H_6, C_2H_6O, C_2O, C_3, C_3H_4, C_3H_6, C_3H_6O, C_3H_8, C_3O_2, C_4H_4, C_4H_6, C_4H_8, $C_4H_8O_2$, C_5, H, H_2, H_2O, H_2O_2, OH, O, O_2, O_3, TiO, and Ti.

The calculated molar fraction of species of the working gases and precursor solutions and collisions between them were then utilized for the estimation of the thermal transport properties of the plasma jet with and without TiO_2 precursor solutions at constant pressure and temperature. These transport properties are described by the coefficients found in the Boltzmann equation which is calculated by the use of the Chapman-Enskog method [33]. These coefficients are dependent on the collision integrals $\Omega_{ij}^{(l,s)}$ which is defined as [26,33-36].

$$\Omega_{ij}^{(l,s)} = \left(\frac{2\pi k T_{ij}^*}{\mu_{ij}}\right)^{1/2} \int_0^\infty \int_0^\infty e^{-\gamma^2} \gamma^{2s+3} \times (1 - \cos^l \chi)\, b\mathrm{d}b\mathrm{d}\gamma \quad (10)$$

where the reduced relative speed is given by $\gamma = \left(\mu_{ij}/2k_BT\right)^{1/2} g$, χ is the deflection angle, b is the impact parameter, and $\mu_{ij} = m_i m_j/\left(m_i + m_j\right)$ is the reduced mass. All the interaction potentials for the calculation of these collision integrals for each interaction were compiled in the *T & TWinner* [37], a simple software that uses algorithms and contains huge thermochemistry database offered by Science des Procédés Céramiques et de Traitements de Surface (SPCTS) laboratory (now IRCER-Institute for Ceramic Research) and is used by other authors [14,31,38-40].

The transport coefficients considered in this work are dynamic viscosity, thermal conductivity, and electrical conductivity which are necessary for the investigation of the plasma jet's behaviour. Dynamic viscosity characterizes the transport of momentum in plasma [41] which was calculated using the first-order approximation of the Chapman-Enskog method proposed by Hirschfelder *et al.* [36,42]. On the other hand, thermal conductivity controls heat transfer which is a sum of three contributions [43]. The first contribution is the translational thermal conductivity [44] which comprises heavy and electron translational thermal conductivities that were calculated using the second and third approximation, respectively [36,42]. The other two contributions are related to the internal and reaction thermal conductivities. The electrical conductivity, moreover, is the transport of mass of electrons and ions caused by the concentration, temperature and pressure gradients [45] and it is calculated using the third approximations proposed by Devoto [36,41,42,46].

The required collision integrals for the interactions between different species were estimated using interaction potentials from the reference methods within the software [37]. The following are the collisions between species within the plasma jet that determine its transport properties: (i) neutral-neutral interactions, (ii) electron-neutral interactions, (iii) neutral-ion interactions, and (iv) ion-ion interactions [19]. Once these collision integrals were calculated versus temperature, they were fitted obtaining a system of linear equations that can be suitably solved to obtain the different transport properties being considered. The fitting was made on values corresponding to temperatures varying between 300 K and 20,000 K with a 100 K step. The calculation of transport coefficients was limited to 20,000 K since the temperatures of the spraying plasma jets were limited to 16,000 K. The molar quantity of the considered species and transport coefficients of the different plasma mixtures were stored in files.

In this work, the modified ability of the heating factor (AHF) which describes the ability of the working gas to melt the solution particles during the SPPS process was calculated. It was first supplemented by Pawlowski [47] showing only the dynamic viscosity and thermal conductivity. Assuming a particle having only a single temperature in a gas having also one temperature, the heat transfer from plasma to particle is given by the following equation:

$$\pi d_{\mathrm{p}}^2 h(T_{\mathrm{g}} - T_{\mathrm{p}}) = (1/6)\pi \rho_{\mathrm{p}} c_{\mathrm{p}} d_{\mathrm{p}}^3 (dT_{\mathrm{p}}/dt) \quad (11)$$

where d_{p}-diameter of particle, T_{g}- temperature of gas, T_{p}-temperature of particle, ρ_{p}- density of particle, and c_{p}- its specific heat. The term at the left is the transferred energy from plasma which is related to the AHF parameter while the term at the right describes the energy absorbed by particle. After consideration of the conditions presented in [31] and [47], the final calculations were modified to only take the transport coefficients and are expressed as:

$$\frac{1}{(T_{\mathrm{g}}-300)}\left(AHF \cdot \frac{v_{\mathrm{g}}}{L}\right)^{1/2} = \frac{\langle \lambda_{\mathrm{g}} \rangle}{\sqrt{\langle \eta_{\mathrm{g}} \rangle}} \quad (12)$$

where v_{g}- velocity of gas, L- length of high-temperature zone of the plasma jet, $\langle \lambda_{\mathrm{g}} \rangle$- average thermal conductivity of gas, and $\langle \eta_{\mathrm{g}} \rangle$- average dynamic viscosity of gas.

RESULTS AND DISCUSSIONS

Effects of Solution Precursor on Transport Coefficients

The thermal transport properties of the Ar + H_2 working gases were calculated as well as their modified AHF values when different TiO_2 precursor solutions were added. When these solutions were introduced to the pure Ar + H_2 working gases, the thermal properties of the working gases were altered. They are caused by the disappearance of molecular and atomic particles and are controlled only by collisions between ionized species.

In Fig. 1, the molar fraction of major species of the Ar + H_2 plasma working gas mixture is shown when the different precursor solutions were added. The first half of the plasma temperature was governed by heavy particles and neutral atoms, while the second half was controlled by the most charged species. The decomposition of the solution into molecules took place at temperatures below 4000 K. At temperatures between 4000-5900 K, the decomposition of molecules into atoms took place. When the temperature rises further, the ionization of atoms occurs. The precursor decomposition to TiO_2 occurs at lower temperatures with a very low molar fraction compared to the pure working gas mixture making it insignificant for thermal transport estimations. Titanium atoms ionize first since Ti has the lowest ionization potential, followed by carbon atoms, then hydrogen atoms, and finally argon atoms (~6.8 eV for Ti, ~11.28 for C, ~13.59 eV for H, and ~15.7 eV for Ar).

Figure 1 also depicts the evolution of the mole quantities of species common in plasma in the presence of TiO_2 precursor solutions. The dissociation of the TIP and TB precursor solutions with C_2H and C_2H_2 as intermediate products leads to a rapid increase in the density of H, which consequently becomes the most abundant species in the plasma. The concentration of atomic carbon also increases as a result of the continuous dissociation of carbon molecules. These observations have not been clearly seen when the TiN precursor solution was used. In addition, for all plasma mixtures, the ionization reactions continuously increase the number of electrons up to 20,000 K, with hydrogen ions being one of the dominant species in the plasma. Analyzing the behavioral patterns of the plasma, it is expected that in addition to Ar and Ar^+, the gas properties were dominated by e^-, H, H^+, C, and C^+ pairs. The use of TIP and TB precursors using the solvents water and ethanol increased the number of e^-, H, H^+, C, and C^+ species within the plasma resulting in higher deviations of transport properties than when using the TiN precursor. Evidently, the thermal transport properties of the working gases depend on the species that make up the plasma.

Dynamic viscosity. For the Ar + H_2 plasma working gases alone, the dynamic viscosity agrees well with the data from the literature [14, 32]. At constant pressure, the maximum viscosity was reached at about 10,500 K, as illustrated in Fig. 2. Above this temperature, a decrease in the dynamic viscosity was observed as molecules and atoms continuously disappear [41] and, remarkably, ionization occurs as the collision integrals for Coulomb interactions between neutral species become lesser than those for interactions between charged species [24].

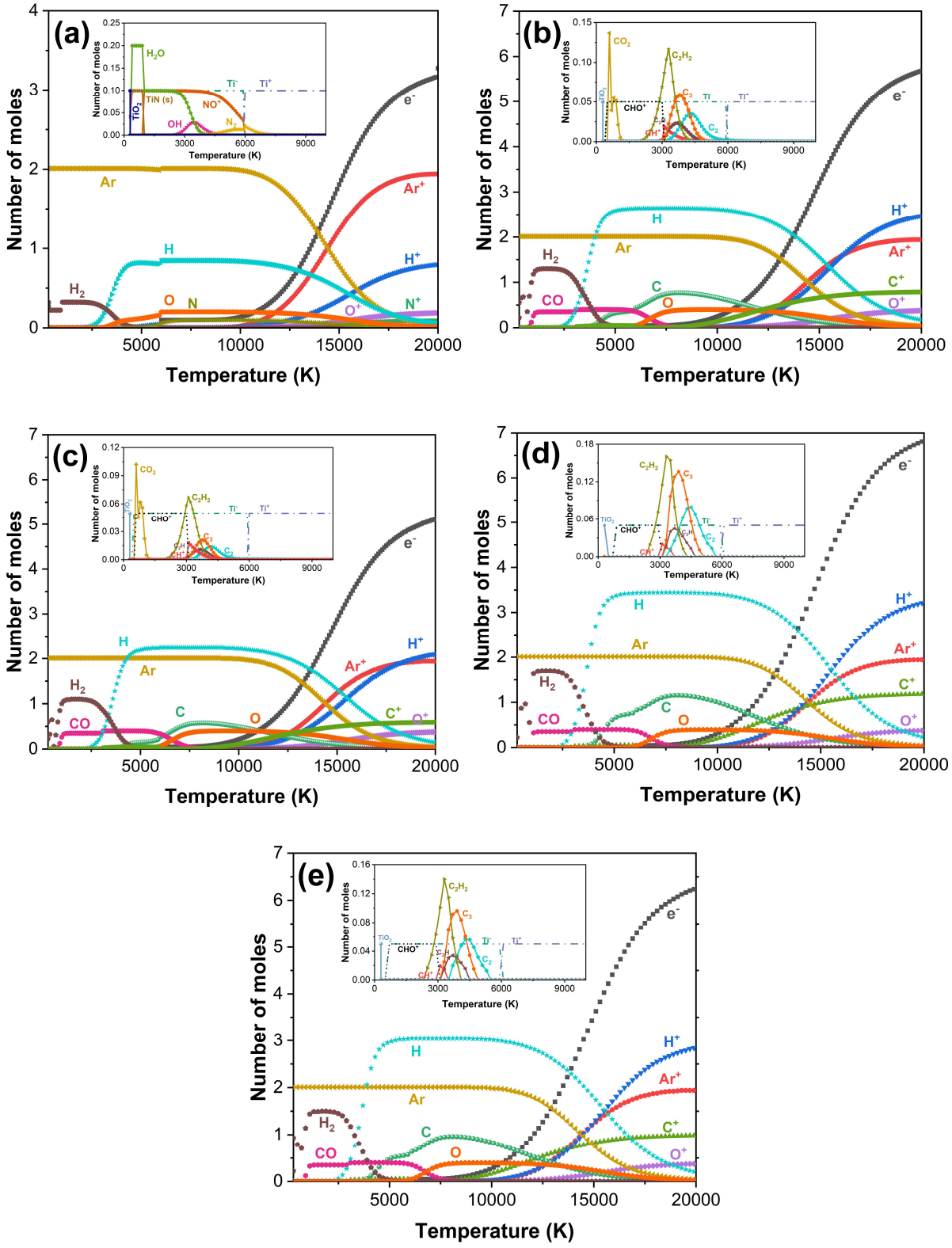

Fig. 1. Molar fraction of different species within plasma mixtures of Ar + H_2 + (a) TiN + water, (b) TB + water, (c) TIP + water, (d) TB + ethanol, and (e) TIP + ethanol at 1.0 M solution concentration and injected at 50 ml min^{-1} feed rate.

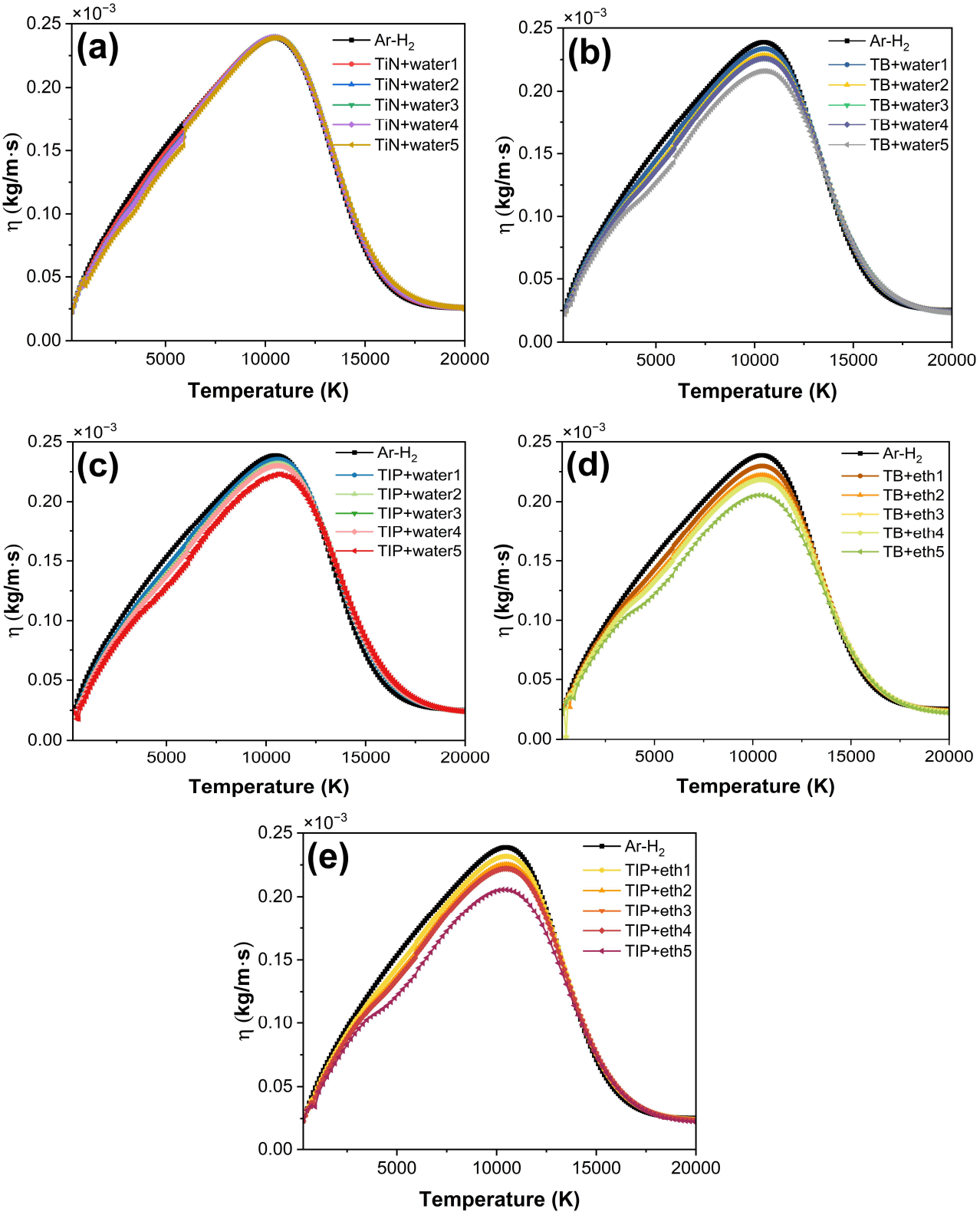

Fig. 2. Dynamic viscosities of Ar + H_2 plasma with the presence of (a) TiN + water, (b) TB + water, (c) TIP + water, (d) TB + ethanol, and (e) TIP + ethanol.

The dynamic viscosity of the plasma jet was affected and lowered by the presence of the precursor solutions TB and TIP, indicating that the momentum of the particles in the plasma jet was also reduced. The solution with the highest concentration (1.0 M) injected at the highest feed rate (50 ml min^{-1}) showed the lowest viscosity of the plasma. Among the three precursor solutions, TB + eth5 showed the lowest peak at 10,500 K with a difference of 0.23×10^{-4} kg m^{-1} s^{-1} from the viscosity of the pure Ar + H_2 working gases, which may lead to a remarkable improvement in the modified AHF of the plasma jet. The addition of TiN showed no significant difference compared to the addition of TIP and TB, regardless of the feed rate and concentration. This may have less impact on the estimate of the modified AHF for this type of plasma jet (see Section 3.2.3).

Thermal conductivity. Two major peaks were observed in the thermal conductivity of pure Ar + H_2 working gases as shown in Fig. 3, and this is in good agreement with other reported works [14,31]. The first peak was mainly due to the dissociation of the H_2 molecule, as evidenced by the fact that an Ar + H_2 mixture contains less hydrogen. The second peak at about 15,000 K was due to the further reaction thermal conductivity and corresponds to the maximum ionization of Ar to Ar^+ and H to H^+ [34,35,41].

It was observed that the thermal conductivity increased when the different TiO_2 precursor solutions were added to Ar + H_2 working gases, as shown in Fig. 3. In the first place, the water decomposition into atomic hydrogen and oxygen starts at 3,000 K [14]. The atomic hydrogen is in fact excited in the plasma environment, which leads to an increase in mobility, *i.e.*, the thermal conductivity of the plasma jet. It was also noted that additional hydrogens were dissociated from the TIP and TB precursor solutions, which increased the number of mobile atomic species, hence, an increase in thermal conductivity was observed. The factors for this phenomenon were the existence of large reaction thermal conductivity and the contributed collision integrals for the interactions between the hydrogen species. This lead to the conclusion that an additional amount of hydrogen produces a large difference in thermal conductivity at temperatures around 3,500 K [35]. However, lower thermal conductivity was obtained upon the addition of TiN precursor solution compared to the other two precursors. This was because TiN does not contain hydrogen atom and only water as solvent provides H_2 to be dissociated as presented in Eqs. (1) to (9).

In addition, there was a sudden drop in the curve at about 6000 K with a discontinuity, corresponding to the conversion of Ti^- to Ti^+ from the three precursors. Moreover, when TIP and TB precursor solutions were introduced, a peak appeared at about 6500 K and this was due to the decomposition of the organic compounds to C and O, which was also reported in the literature [27,48]. The decomposition of these organic compounds produced highly excited atoms that were not found when the TiN precursor solution was added.

Electrical conductivity. The electrical conductivity depends on the electron density and inversely on the ionic collision frequency which hinders the transport of current [28,49]. As presented in Fig. 1, the H^+ and electron number densities were increased with the addition of TiO_2 precursor solution. In a plasma where the degree of ionization is low, collisions between charged and neutral particles dominate. It has been reported that electron-neutral collisions have a strong influence on the electrical conductivity of the plasma [49,50]. Figure 4 shows the influence of electron-neutral collisions on the electrical conductivity of the Ar + H_2 plasma jet for different mixtures. As can be seen, the addition of TiO_2 precursor solution considerably increased the electrical conductivity between 6,000 K and 11,000 K. This indicates that the Ar + H_2 plasma working gases in the presence of TiO_2 precursor solution exhibit the desirable properties of high conductivity in this temperature range. Above this temperature range, the degree of ionization is high and charged particle collisions dominate causing the electrical conductivity to continually increase. An increase in electron temperature leads to a decrease in the frequency of electron-electron collisions and consequently to an increase in conductivity. However, at temperatures above 11,000 K, the addition of various TiO_2 solutions regardless of feed rate and concentration, caused no significant changes in the electrical conductivity compared to pure Ar+H_2 plasma. This is because the electrical conductivity at higher temperatures depends weakly on the nature of species [50]. The contribution of electron-neutral collision becomes negligible at a high degree of ionization and therefore the electrical conductivity becomes independent of the kind of gas [49].

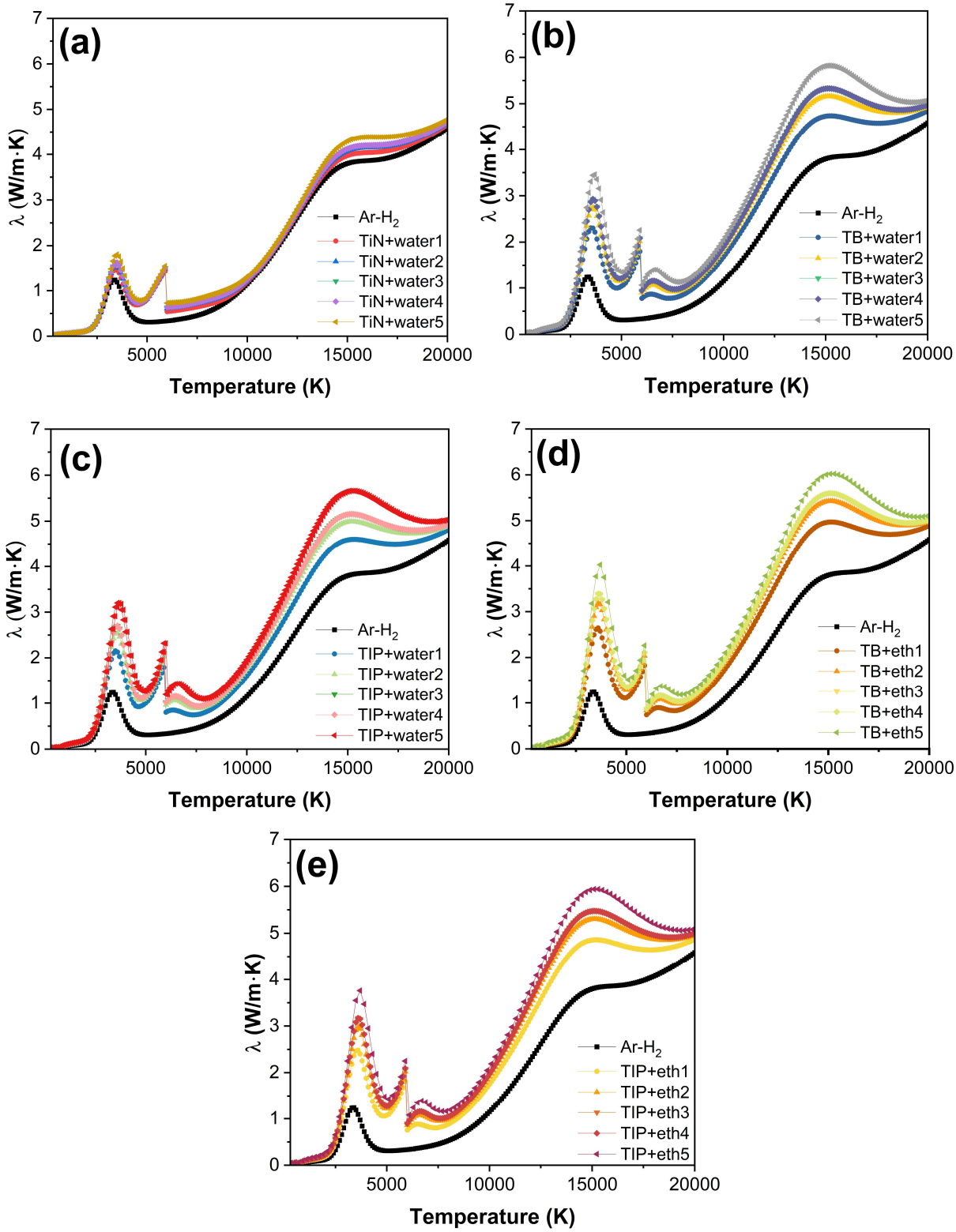

Fig. 3. Thermal conductivities of Ar + H_2 plasma with the presence of (a) TiN + water, (b) TB + water, (c) TIP + water, (d) TB + ethanol, and (e) TIP + ethanol.

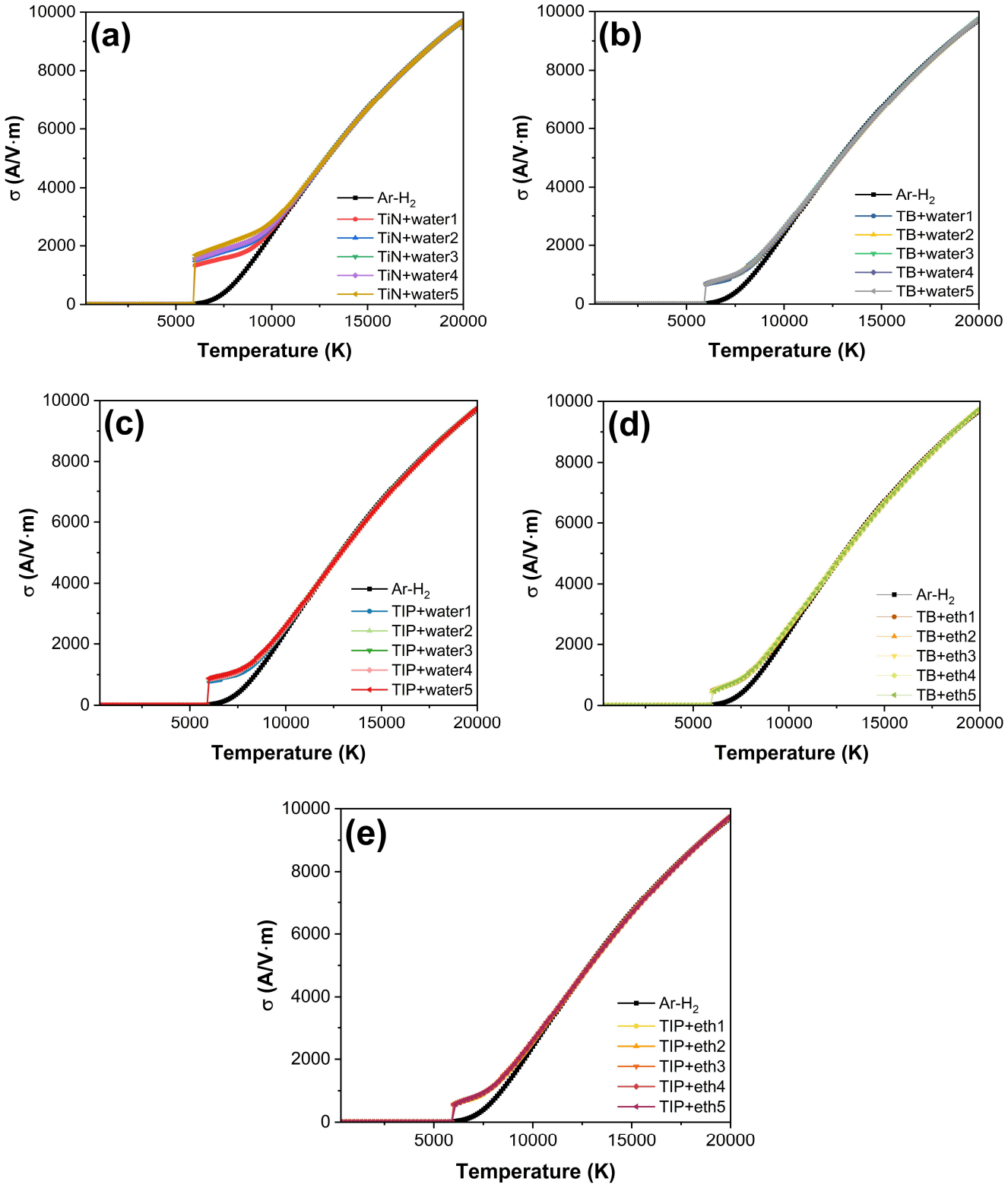

Fig. 4. Electrical conductivities of Ar+H_2 plasma with the presence of (a) TiN + water, (b) TB + water, (c) TIP + water, (d) TB + ethanol, and (e) TIP + ethanol.

Effects of Solution Concentration and Feed Rate on Transport Coefficients

The deviations of the transport properties were due to the different TiO_2 solutions with different concentration and feed rate. It can be observed that the thermal conductivity was strongly influenced by the solution feed rate and its concentration. The higher the feed rate and solution concentration, the higher the increase in thermal conductivity. The successive increase in the peak thermal conductivity values and the decrease in the dynamic viscosity of the plasma working gases were due to the increased solution concentration and feed rate. Increasing concentration tends to increase the reaction rate. The reason for this trend also has to do with collisions. A higher concentration means that more reactant particles are closer together, exposed to more collisions, and have a greater chance of reacting. Also, an increase in the rate of feeding the solution to the plasma means an increase in the volume of solution that must be delivered in a given time period. The number of species involved in the reactions has increased, resulting in a higher number of collisions.

Considering that the solvent is water and the precursors $Ti(OC_3H_7)_4$ and $Ti(OC_4H_9)_4$ have dissociated hydrogen atoms when heat was applied, the conclusion of the reference work [14] is still valid. The results for electrical conductivity did not show any differences for different concentrations and feed rates of TiO_2 precursor solutions. The thermal conductivity and dynamic viscosity clearly project deviations when the concentration and feed rate of TiO_2 precursor solutions were varied. Since the mobility of electrons was higher than that of charged species, only the electron's contribution was considered in the estimation of electrical conductivity. The electrical conductivity curves showed a trend similar to that reported in the literature [34,50-52]. However, discontinuities in the curves were observed which usually occur in a two-temperature plasma [52,53]. This discontinuity at ~6,000 K was also compared to the discontinuity found in the thermal conductivity curve in the presence of TiO_2 precursor solution. At this temperature, there was a sudden shift of ionized Ti from Ti^- to Ti^+ and thus the thermal transport properties were strongly dependent on the equilibrium composition.

Modified AHF. The estimated modified AHF for the gases of different compositions is shown in Fig. 5. From the thermal transport properties, the modified AHF of Ar + H_2 plasma working gases was improved in the presence of various TiO_2 precursor solutions. A marked increment of thermal conductivity was observed when different TiO_2 precursor solutions were present during solution plasma spraying, as well as the ability of heating factor of the plasma jet based on the definition of modified AHF (Eq. (12)). The highest modified AHF values were obtained for the compositions with the TB precursor solution, which are 2 to 3.5 times higher than those with pure Ar + H_2 plasma working gases. Among the three TiO_2 precursors, TB has the highest content of decomposed molecular hydrogen. High hydrogen content in the plasma working gases increased the thermal conductivity of the plasma jet [35] due to hydrogen excitement and increased mobility in the high-temperature environment, thus, increasing the modified AHF of the plasma in the SPPS technique. This remarkable increase in modified AHF means a higher heat flux between the plasma jet and the liquid feedstocks, which may greatly alter the phenomena taking place inside the plasma jet core and cause the feedstock particles to undergo considerable chemical and physical transformations during solution plasma spraying. Thus, it is recommended to mainly use a precursor that will significantly modify the plasma working gases during the SPPS process, such as TIP and TB solution precursors, in particular, when producing TiO_2 plasma sprayed coatings.

1. CONCLUSIONS

The thermal transport properties, such as the dynamic viscosity and thermal conductivity, allow for the estimation of heat and momentum transfer between the Ar + H_2 plasma working gases and the TiO_2 precursor solutions of varying feed rates and concentrations. For the TiO_2 precursors used, TB and TIP were found to strongly affect the transport properties of the plasma working gases. The dynamic viscosity of the plasma jet was lowered by the presence of TB and TIP precursor solutions, especially when a high concentration and feed rate were used, while TiN showed no significant effect regardless of the feed rate and concentration. Conversely, the thermal conductivity increases when TB and TIP precursor solutions were present and was greatly influenced by solution concentration and feed rate. The deviation of the transport properties was due to

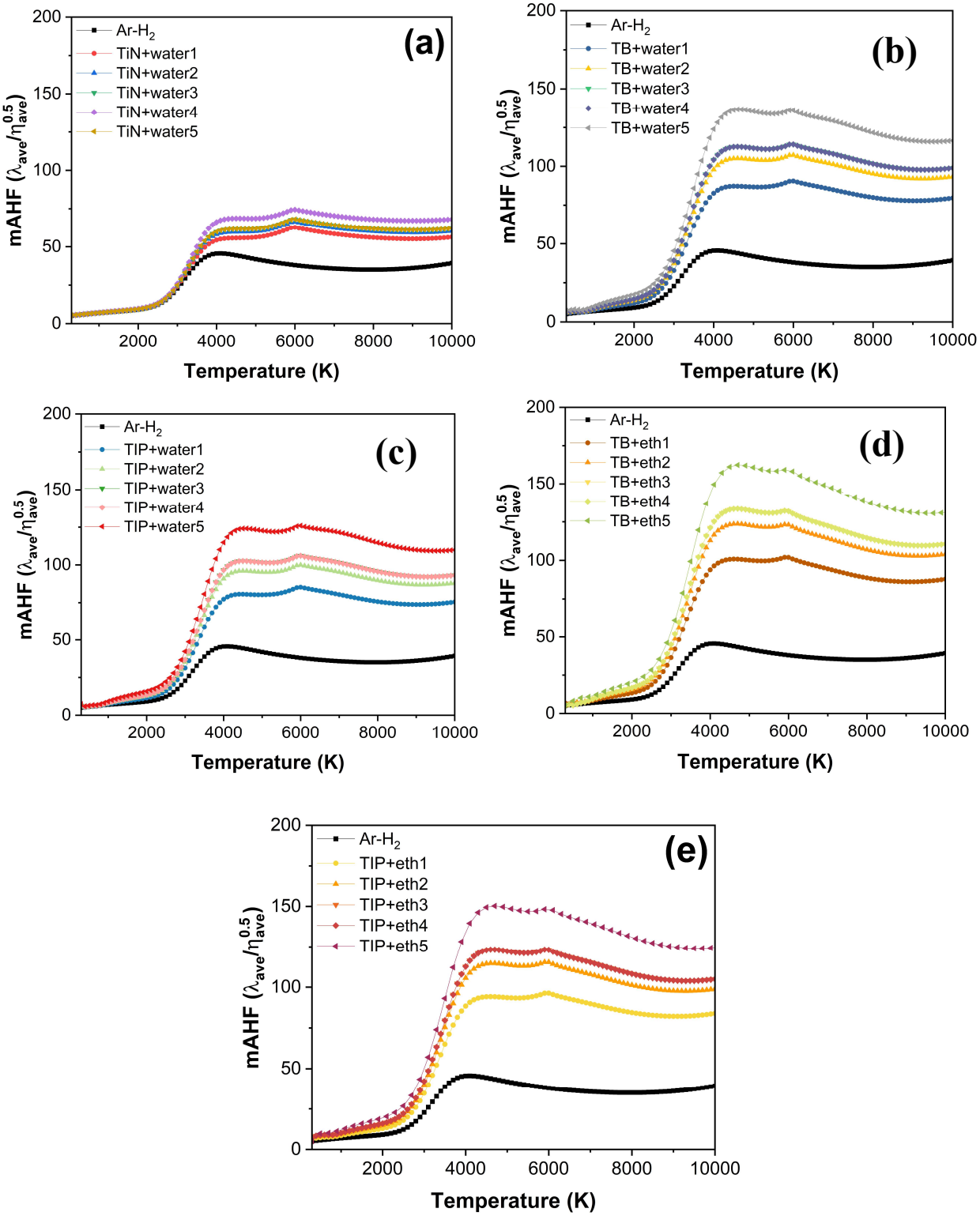

Fig. 5. Modified AHF of Ar + H_2 plasma with the presence of (a) TiN + water, (b) TB + water, (c) TIP + water, (d) TB + ethanol, and (e) TIP + ethanol.

the different TiO_2 solutions with different concentrations and feed rates. The successive increase in the peak thermal conductivity values and the decrease in the dynamic viscosity of the plasma working gases were due to increased solution concentration and feed rate. This was attributed to the additional hydrogen ions in TIP and TB precursor solutions which increase the number of mobile atomic species which are absent in the TiN precursor. Regardless of the solution concentration and feed rate, the electrical conductivity was also modified when various TiO_2 precursor solutions were added. From the transport coefficients, the modified AHF values of the plasma working gases were increased in the presence of different TiO_2 precursor solutions. The highest values were achieved for the compositions including the TB precursor solution which are 2 to 3.5 times greater than for pure $Ar+H_2$ plasma working gases. These findings suggest that both TB and TIP are potential precursors for the solution precursor plasma spaying of TiO_2 coatings.

ACKNOWLEDGMENTS

The authors thank the Department of Research-OVCRE of MSU-IIT and DOST-PCIEERD for supporting this research. Ms. Key T. Simfroso and Mr. Alfredo Q. Liboon, Jr. acknowledge DOST-ASTHRDP for the scholarship grant. Bernard Pateyron is greatly acknowledged for his expertise in the use of *T&TWinner* software and insights into the results.

REFERENCES

[1] Vasiliev, A. L.; Padture N. P., Coatings of Metastable Ceramics Deposited by Solution-Precursor Plasma Spray: II. Ternary ZrO_2-Y_2O_3-Al_2O_3 System. *Acta Mater.* **2006**, *54*, 4921-4928, DOI: 10.1016/j.actamat.2006.06.026.

[2] Parukuttyamma, S. D.; Margolis, J.; Liu, H.; Grey, C. P.; Sampath, S.; Herman, H.; Parise, J. B., Yttrium Aluminum Garnet (YAG) Films through a Precursor Plasma Spraying Technique. *J. Am. Ceram. Soc.* **2001**, *84* (8), 1906-908, DOI: 10.1111/j.1151-2916.2001.tb00935.x.

[3] Xie, L.; Ma, X.; Jordan, E. H.; Padture, N. P.; Xiao, D. T.; Gell, M., Identification of coating deposition mechanisms in the solution-precursor plasma-spray process using model spray experiments. *Mater. Sci. Eng. A.* **2003**, *362*, 204-212, DOI: 10.1016/S0921-5093(03)00617-8.

[4] Karthikeyan, J.; Berndt, C. C.; Tikkanen, J.; Wang, J. Y.; King, A. H.; Herman, H., Preparation of Nanophase Materials by Thermal Spray Processing of Liquid Precursors. *Nanostruct. Mater*. **1997**, *9*, 137-140, DOI: 10.1016/S0965-9773(97)00037-8.

[5] Xie, L.; Ma, X.; Jordan, E. H.; Padture, N. P.; Xiao, D. T.; Gell, M., Deposition of thermal barrier coatings using the solution precursor plasma spray process. *J. Mater. Sci.* **2004**, *39*, 1639-1646, DOI: 10.1023/B:JMSC.0000016163.81534.19.

[6] Padture, N. P.; Schlichting, K. W.; Bhatia, T.; Ozturk, A.; Cetegen, B.; Jordan, E. H.; Gell, M.; Jiang, S.; Xiao, T. D.; Strutt, P. R.; Garcia, E.; Miranzo, P.; Osendi, M. I., Towards Durable Thermal Barrier Coatings With Novel Microstructures Deposited By Solution-Precursor Plasma Spray. *Acta Mater.* **2001**, *49*, 2251-2257, DOI: 10.1016/S1359-6454(01)00130-6.

[7] Zhang, C.; Geng, X.; Olivier, M.; Liao, H.; Debliquy, M., Solution precursor plasma-sprayed tungsten oxide coatings for nitrogen dioxide detection. *Ceram. Int.* **2014**, *40*, 11427-11431, DOI: 10.1016/j.ceramint.2014.03.109.

[8] Coyle, T. W.; Garcia, E.; Zhang, Z.; Gan, L., Plasma Spray Deposition of Hydroxyapatite Coatings from Sol Precursors. *Mater. Sci. Forum*. **2007**, *539-543*, 1128-1133, DOI: 10.4028/www.scientific.net/MSF.539-543.1128.

[9] Oseghe, E. O.; Ndungu, P. G.; Jonnalagadda, S. B., Synthesis, Characterization, and Application of TiO_2 Nanoparticles-Effect of pH Adjusted Solvent. *J. Adv. Oxid. Technol.* **2015**, *18* (2), 253-263, DOI: 10.1515/jaots-2015-0211.

[10] Qourzal, S.; Tamimi, M.; Assabbane, A.; Bouamrane, A.; Nounah, A.; Laânab, L.; Ait-Ichou, Y., Preparation of TiO_2 Photocatalyst Using $TiCl_4$ as a Precursor and its Photocatalytic Performance. *J. Appl. Sci.* **2006**, *6* (7), 1553-1559, DOI: 10.3923/jas.2006.1553.1559.

[11] Wang, W. Z.; Coyle, T.; Zhao, D., Preparation of Lanthanum Zirconate Coatings by the Solution Precursor Plasma Spray. *J. Therm. Spray Technol.*

2014, *23* (5), 827-832, DOI: 10.1007/s11666-014-0084-3.

[12] Saha, A.; Seal, S.; Cetegen, B.; Jordan, E.; Ozturk, A.; Basu, S., Thermo-physical processes in cerium nitrate precursor droplets injected into high temperature plasma. *Surf. Coat. Technol.* **2009**, *203*, 2081-209, DOI: 10.1016/j.surfcoat.2008.09.018.

[13] Castillo, I.; Munz, R. J., Transient heat, mass and momentum transfer of an evaporating stationary droplet containing dissolved cerium nitrate in a rf thermal argon-oxygen plasma under reduced pressure. *Int. J. Heat Mass Transf.* **2007**, *50* (1-2), 240-256, DOI: 10.1016/j.ijheatmasstransfer.2006.06.023.

[14] Carpio, P.; Pawłowski, L.; Pateyron, B., Numerical investigation of influence of precursors on transport properties of the jets used in solution precursor plasma spraying. *Surf. Coat. Technol.* **2019**, *371*, 131-135, DOI: 10.1016/j.surfcoat.2018.09.073.

[15] Chen, D.; Jordan, E. H.; Gell, M., Porous TiO_2 coating using the solution precursor plasma spray process. *Surf. Coat. Technol.* **2008**, *202*, 6113-6119, DOI: 10.1016/ j.surfcoat.2008.07.017.

[16] Chen, D.; Jordan, E. H.; Gell, M.; Wei, M., Apatite formation on alkaline-treated dense TiO_2 coatings deposited using the solution precursor plasma spray process. *Acta Biomater.* **2008**, *4*, 553-559, DOI: 10.1016/j.actbio.2007.11.008.

[17] Chen, D.; Jordan, E. H.; Gell, M.; Ma, X., Dense TiO_2 Coating Using the Solution Precursor Plasma Spray Process. *J. Am. Ceram. Soc.* **2008**, *91* (3), 865-872, DOI: 10.1111/j.1551-2916.2007.02225.x.

[18] Wen, K.; Liu, M.; Liu, X.; Deng, C.; Zhou, K., Deposition of Photocatalytic TiO_2 Coating by Modifying the Solidification Pathway in Plasma Spraying. *Coatings*, **2017**, *7* (169), 9 pages, DOI: 10.3390/coatings7100169.

[19] Zhang, X. N.; Li, H. P.; Murphy, A. B.; Xia, W. D., Comparison of the transport properties of two-temperature argon plasmas calculated using different methods. *Plasma Sources Sci. Technol.* **2015**, *24*, 1-17, DOI: 10.1088/0963-0252/24/3/035011.

[20] Wu, Y.; Chen, Z.; Yang, F.; Cressault, Y.; Murphy, A. B.; Guo, A.; Liu, Z.; Rong, M.; Sun, H., Two-temperature thermodynamic and transport properties of SF_6-Cu plasmas. *J. Phys. D: Appl. Phys.* **2015**, *48*, 1-25, DOI: 10.1088/0022-3727/48/41/415205.

[21] Wang, H.; Wang, W.; Yan, J. D.; Qi, H.; Geng, J.; Wu, Y., Thermodynamic properties and transport coefficients of a two-temperature polytetrafluoroethylene vapor plasma for ablation-controlled discharge applications. *J. Phys. D: Appl. Phys.* **2017**, *50*, 395204, 1-14, DOI: 10.1088/1361-6463/aa7d68.

[22] Boulos, M. I.; Fauchais, P. L.; Pfender, E., *Transport Properties of Non-Equilibrium Plasmas*. In: Handbook of Thermal Plasmas, Springer, **2015**, 1-43, DOI: 10.1007/978-3-319-12183-3_10-1..

[23] Grishin, Yu. M.; Kozlov, N. P.; Skryabin, A. S., Efficiency of the Plasma-Chemical Method of Preparation of Silicon from Quartz in an Argon-Hydrogen Flow. *High Temp.* **2016**, *54* (5), 619-626, DOI: 10.1134/S0018151X16040088.

[24] Murphy, A. B.; Tam, E., Thermodynamic properties and transport coefficients of arc lamp plasmas: argon, krypton and xenon. *J. Phys. D: Appl. Phys.* **2014**, *47*, 1-10, DOI: 10.1088/0022-3727/47/29/295202.

[25] Wang, C.; Wu, Y.; Chen, Z.; Yang, F.; Feng, Y.; Rong, M.; Zhang, H., Thermodynamic and Transport Properties of Real Air Plasma in Wide Range of Temperature and Pressure. *Plasma Sci. Technol.* **2016**, *18* (7), 732-739, DOI: 10.1088/1009-0630/18/7/06.

[26] Li, X.; Guo, X.; Murphy, A. B.; Zhao, H.; Wu, J.; Guo, Z., Calculations of thermodynamic properties and transport coefficients of $C_5F_{10}O$-CO_2 thermal plasmas. *J. Appl. Phys.* **2017**, *122*, 1-11, DOI: 10.1063/ 1.5006635.

[27] Lisong, Z.; Mingtian, Y.; Lei, P.; Qiaogen, Z., Thermodynamic properties and transport coefficients of C_4F_7N/CO_2 thermal plasma as an alternative to SF_6. *IEEE Int. Pulsed Power Plasma Sci. (PPPS)*. **2019**, 1-4, DOI: 10.1109/PPPS34859.2019.9009981.

[28] Colonna, G.; D'Angola, A.; Pietanza, L. D.; Capitelli, M.; Pirani, F.; Stevanato, E.; Laricchiuta, A., Thermodynamic and transport properties of plasmas including silicon-based compounds. *Plasma Sources Sci. Technol.* **2018**, *27*, 11, DOI: 10.1088/1361-6595/aa9f9b.

[29] Miao, L.; Grishin, Yu, M., Studies of vortex

characteristics and gas-dynamic fields in Ar-H_2 inductively coupled plasma", *Int. J. Heat Mass Transf.* **2019**, *144*, 12, DOI: 10.1016/j.ijheatmasstransfer.2019.118671.

[30] Miao, L.; Grishin, Yu, M., Gas dynamic-thermal-concentration fields and evaporation process of quartz particles in Ar–H_2 inductively coupled plasma. *Plasma Sources Sci. Technol.* **2020**, *29*, 13 pages, DOI: 10.1088/1361-6595/ab8e4a.

[31] Pateyron, B.; Calvé, N.; Pawłowski, L., Influence of water and ethanol on transport properties of the jets used in suspension plasma spraying. *Surf. Coat. Technol.* **2013***, 220*, 257-260, DOI: 10.1016/j.surfcoat.2012.10.010.

[32] White, W. B.; Johnson, S. M.; Dantzig, G. B., Chemical Equilibrium in Complex Mixtures. *J. Chem. Phys.* **1958**, *28* (50), 751-755, DOI: 10.1063/1.1744264.

[33] Hirschfelder, J. O.; Curtis, C. F.; Bird, R. B., *Molecular Theory of Gases and Liquids* 2nd edn, New York Wiley, **1964**.

[34] Murphy, A. B.; Arundell, C. J., Transport Coefficients of Argon, Nitrogen, Oxygen, Argon-Nitrogen, and Argon-Oxygen Plasmas. *Plasma Chem. Plasma Process.* **1994**, *14* (4), 451-489, DOI: 10.1007/BF01570207.

[35] Murphy, A. B., Transport Coefficients of Hydrogen and Argon-Hydrogen Plasmas. *Plasma Chem. Plasma Process.* **2000**, *20* (3), 279-297, DOI: 10.1023/A:1007099926249.

[36] Yang, A.; Liu, Y.; Sun, B.; Wang, X.; Cressault, Y.; Zhong, L.; Rong, M.; Wu, Y.; Niu, C., Thermodynamic properties and transport coefficients of high-temperature CO_2 thermal plasmas mixed with C_2F_4. *J. Phys. D: Appl. Phys.*, **2015**, *48*, 25 pages, DOI: 10.1088/0022-3727/48/49/495202.

[37] Pateyron, B., *T&TWinner*. http://ttwinner.free.fr.

[38] Cañas, E.; Vicent, M.; Orts, M. J.; Sánchez, E., Bioactive glass coatings by suspension plasma spraying from glycolether-based solvent feedstock. *Surf. Coat. Technol.* **2016**, *318*, 190-197, DOI: 10.1016/j.surfcoat.2016.12.060.

[39] Gueye, P.; Cressault, Y.; Rohani, V.; Fucheri, L., A simplified model for the determination of current-voltage characteristics of a high pressure hydrogen plasma arc. *J. App. Phys.* **2017**, *121* (7), 11 pages, DOI: 10.1063/1.4976572.

[40] Aissa, A.; El Ganaoui, M.; Sahnoun, M., Numerical investigation of heat and momentum transfer to particles in high temperature thermal spraying. *Eur. Phys. J. Appl. Phys.*, **2017**, *78* (3), 6 pages, DOI: 10.1051/epjap/2017160492.

[41] Kagoné, A. K.; Koalaga, Z.; Zougmore, F., Calculation of air-water vapor mixtures thermal plasmas transport coefficients. *IOP Conf. Ser.: Mater. Sci. Eng.* **2012**, *29*, 15 pages, DOI: 10.1088/1757-899X/29/1/012004.

[42] Pateyron, B.; Elchinger, M.-F.; Delluc, G.; Fauchais, P., Thermodynamic and Transport Properties of Ar-H_2 and Ar-He Plasma Gases Used for Spraying at Atmospheric Pressure. I: Properties of the Mixtures. *Plasma Chem. Plasma Process.* **1992**, *12* (4), 421-448, DOI: 10.1007/BF01447253.

[43] Pateyron, B.; Delluc. G.; Fauchais, P., Chemical and Transport Properties of Carbon-Oxygen-Hydrogen Plasmas in Isochoric Conditions. *Plasma Chem. Plasma Process.* **2005**, *25* (5), 485-502, DOI: 10.1007/s11090-005-4994-1.

[44] Capitelli, M.; Gorse, C.; Fauchais, P., Transport Coefficients of High Temperature N_2-H_2 Mixtures. *J. Phys.* **1977**, *38*, 653-657, DOI: 10.1051/jphys:01977003806065300.

[45] Capitelli, M.; Colonna, G.; Gorse, C.; D'Angola, A., Transport properties of high temperature air in local thermodynamic equilibrium. *Eur. Phys. J. D.* **2000**, *11*, 279-289, DOI: 10.1007/s100530070094.

[46] Devoto, R. S., Transport coefficients of ionized argon. *Phys. Fluids.* **1973**, *16* (5), 616-623, DOI: 10.1063/1.1694396.

[47] Pawlowski, L. The Science and Engineering of Thermal Spray Coatings 2nd edn, Wiley, Chichester: **2008**, p. 197.

[48] Yang, A.; Liu, Y.; Zhong, L.; Wang, X.; Niu, C.; Rong, M.; Han, G.; Zhang, Y.; Lu, Y.; Wu, Y., Thermodynamic Properties and Transport Coefficients of CO_2-Cu Thermal Plasmas. *Plasma Chem. Plasma Process.* **2016**, *36* (4), 1141-1160, DOI: 10.1007/s11090-016-9709-2.

[49] Erwin, D. A.; Kunc, J. A., Electron temperature and ionization degree dependence of electron transport

coefficients in monatomic gases. *Phys. Fluids.* **1985**, *28*, 3349-3355, DOI: 10.1063/1.865334.

[50] Cressault, Y.; Gleizes, A., Thermodynamic properties and transport coefficients in Ar-H_2-Cu plasmas. *J. Phys. D: Appl. Phys.* **2004**, *37*, 560-572, DOI: 10.1088/0022-3727/37/4/008.

[51] Murphy, A. B., Transport Coefficients of Helium and Argon-Helium Plasmas. *IEEE Trans. Plasma Sci.* **1997**, *25* (5), 809-814, DOI: 10.1109/27.649574.

[52] Rat, V.; André, P.; Aubreton, J.; Elchinger, M. F.; Fauchais, P.; Lefort, A., Two-Temperature Transport Coefficients in Argon-Hydrogen Plasmas-II: Inelastic Processes and Influence of Composition. *Plasma Chem. Plasma Process.* **2002**, *22* (4), 475-493, DOI: 10.1023/A:1021363328138.

[53] Rat, V.; Aubreton, J.; André, P.; Elchinger, M. F.; Fauchais, P.; Lefort, A., Transport coefficients in non-equilibrium argon-hydrogen thermal plasmas. *7th European Conference on Thermal Plasma Processes*, France, **2003**, 269-274.